

# Spatial carrier interferometry from $M$ temporal phase shifted interferograms: *Squeezing Interferometry*

M. Servin,<sup>1,\*</sup> M. Cywiak,<sup>1</sup> D. Malacara-Hernandez,<sup>1</sup> J. C. Estrada,<sup>1</sup>  
and J. A. Quiroga,<sup>2</sup>

<sup>1</sup>Centro de Investigaciones en Óptica A.C., Loma del Bosque 115, C.P. 37000., León, Guanajuato, México.

<sup>2</sup>Universidad Complutense de Madrid, Departamento de Óptica, Madrid 2841, Spain

\*Corresponding author: [mservin@cio.mx](mailto:mservin@cio.mx)

**Abstract:** It is well known that having 3 temporal phase shifting (PS) interferograms we do not have many possibilities of using an algorithm with a desired frequency spectrum, detuning, and harmonic robustness. This imposes severe restrictions on the possibilities to demodulate such set of temporal interferograms. It would be nice to apply for example a 7 step PS algorithm to these 3 images in order to have more possibilities to phase demodulate them; even further, it would be even better to apply a quadrature filter having a spatial spread given by a real number to these 3 interferograms. In this paper we propose to do just that; namely we show how to demodulate a set of  $M$ -steps phase shifting images with a quadrature filter having a real-number as spatial spread. The interesting thing in this paper is to use a higher than  $M$  spread quadrature filter to demodulate our interferograms; in traditional PS interferometry one is stuck to the use of  $M$  step phase shifting formula to obtain the searched phase. Using a less than  $M$  PS formula is not interesting at all given that we would not use all the available information. The main idea behind the “squeezing” phase shifting method is to re-arrange the information of the  $M$  phase shifted fringe patterns in such a way to obtain a single carrier frequency interferogram (a spatio-temporal fringe image) and use any two dimensional quadrature filter to demodulate it. In particular we propose the use of Gabor quadrature filters with a spread given by real-numbers along the spatial coordinates. The Gabor filter may be designed in such way that we may squeeze the frequency response of the filter along any desired spatio-temporal dimension, and obtain better signal to noise demodulation ratio, and better harmonic rejection on the estimated phase.

©2008 Optical Society of America

**OCIS codes:** (120.0120) Instrumentation Measurement and Metrology; (120.2650) Fringe Analysis; (120.3180) Interferometry

---

## References and links

1. M. Servin and M. Kujawinska, “Modern fringe pattern analysis in Interferometry,” in *Handbook of Optical Engineering*, D. Malacara and B. J. Thompson eds., (Marcel Dekker, 2001) Chap 14, 373-422.
2. D. Malacara, M. Servin, and Z. Malacara, *Interferogram Analysis for Optical Testing*, (CRC Press, Taylor & Francis, second edition, 2005).
3. K. Freischland and C. L. Koliopoulos, “Fourier description of digital phase measuring interferometry,” *J. Opt. Soc. Am. A* **7**, 542-551 (1990).
4. M. Servin, D. Malacara, D. Marroquin, and F. J. Cuevas, “Complex linear filters for phase shifting with very low detuning sensitivity,” *J. Mod. Opt.* **44**, 1269-1278 (1997).
5. Y. Surrel, “Design of algorithms for phase measurements by the use of phase stepping,” *Appl. Opt.* **35**, 51-60 (1996).
6. M. Takeda, H. Ina, and S. Kobayashi, “Fourier transform methods of fringe-pattern analysis for computer based topography and interferometry,” *J. Opt. Soc. Am. A* **72**, 156-160 (1982).

7. K. H. Womack, "Interferometric phase measurement using spatial synchronous detection," *Opt. Eng.*, **23**, 391-395 (1984).
8. J. H. Bruning, D. R. Herriot, J. E. Gallagher, D. P. Rosenfel, A. D. White, and D. J. Brangaccio, "Digital wavefront measuring interferometry for testing optical surfaces and lenses," *Appl. Opt.* **13**, 2693-2703 (1974).

## 1. Introduction

Phase shifting interferometry (PSI) [1, 2, 8] is typically the first choice or instance for analyzing a wavefront in optical metrology using a laser illuminated interferometer to probe a physical magnitude of interest. Mechanical stability, air turbulence and/or time constraints may sometimes limit the number of phase shifting (PS) interferograms that one may reliably obtain from a given interferometric set-up. As mentioned in the abstract if for some reason we are restricted to a few phase shifted interferograms, let say 3 which is a typical minimum, one is severely restricted by the type PS algorithm that one may use. In mathematical terms we may express this situation as having the following interferograms at our disposal,

$$\begin{aligned}
 I(x, y, -\alpha) &= a(x, y) + b(x, y) \cos[\phi(x, y) - \alpha] \\
 I(x, y, 0) &= a(x, y) + b(x, y) \cos[\phi(x, y)] \\
 I(x, y, +\alpha) &= a(x, y) + b(x, y) \cos[\phi(x, y) + \alpha]
 \end{aligned}
 \tag{1}$$

Having the information displayed in Eq. (1) we do not have too many choices, among them is to use the following formula to obtain  $\phi(x, y)$  as [1],

$$\phi_w(x, y) = \tan^{-1} \left[ \frac{(1 - \cos(\alpha)) [I(x, y, -\alpha) - I(x, y, +\alpha)]}{\sin(\alpha) [2I(x, y, 0) - I(x, y, -\alpha) - I(x, y, +\alpha)]} \right]
 \tag{2}$$

where  $\phi_w(x, y)$  is the phase wrapped version of the true continuous phase  $\phi(x, y)$ . Of course we can use a higher number of phase stepped interferograms and use one of the many techniques available in the literature for PS interferometry [2-5,8], in particular the book of Malacara, *et. al.*, [2] has an exhaustive amount of PS interferometry algorithms.

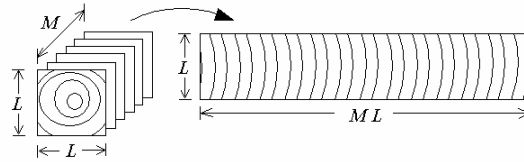


Fig. 1. Schematic of the proposed technique to combine  $M$  phase shifted interferograms of size  $LxL$  into a single-image, spatio-temporal, carrier-frequency image of size  $MLxL$ .

In this work we put forward a technique for transforming  $M$  temporal phase shifted fringe patterns into a *single* image spatio-temporal carrier fringe image [6, 7]. The information re-arrangement herein proposed has several advantages, among them we can use a  $N > M$  phase stepping algorithm to demodulate  $M$  temporal phase shifted interferograms or even better a quadrature filter with any (however fixed) desired spatial spread given by a real number. Assuming that we have  $M$  temporal PS interferograms of size  $LxL$  pixels we will obtain a single carrier frequency fringe pattern of size  $MLxL$  (see Fig. 1) or conversely a single fringe pattern of size  $LxML$  if we decide re-arrange the information along the  $y$  coordinate. In this way the dimensionality of the problem remains unchanged so no information is lost. However using this transformation technique we can have a wider range of fringe processing possibilities, including of course our initial option; which was the standard  $M$  step PS

algorithm. In this work we propose to demodulate our newly formed single-image, spatio-temporal, carrier-frequency fringe pattern of size  $ML \times L$  pixels by means of a two dimensional quadrature Gabor filter.

## 2. Transforming $M$ -PS interferograms into a single spatial carrier fringe pattern

Let us continue with our 3 step phase shifting example. The transformation we are proposing is straightforward; we re-arrange our (by now) three PS fringe patterns to obtain a *single* fringe pattern  $I'(x,y)$  according to the following formula,

$$\left. \begin{aligned} I'(3x, y) &= I(x, y, -\alpha) \\ I'(3x+1, y) &= I(x, y, 0) \\ I'(3x+2, y) &= I(x, y, +\alpha) \end{aligned} \right\} (0,0) \leq (x, y) \leq (L, L) \quad (3)$$

We thus obtain a single spatial carrier frequency fringe pattern  $I'(x,y)$  of size  $3L \times L$  intermixing the three fringe patterns to obtain the single fringe pattern as shown in Fig. 2. If we want to have an evenly spaced sampled spatial carrier interferogram we must restrict the value of the phase step to  $\alpha = 2\pi/3$  in this case. Equivalently we could have had also used the  $y$  coordinate instead, to obtain,

$$\left. \begin{aligned} I'(x, 3y) &= I(x, y, -\alpha) \\ I'(x, 3y+1) &= I(x, y, 0) \\ I'(x, 3y+2) &= I(x, y, +\alpha) \end{aligned} \right\} (0,0) \leq (x, y) \leq (L, L). \quad (4)$$

This is a single-image carrier-frequency interferogram of size  $L \times 3L$  instead.

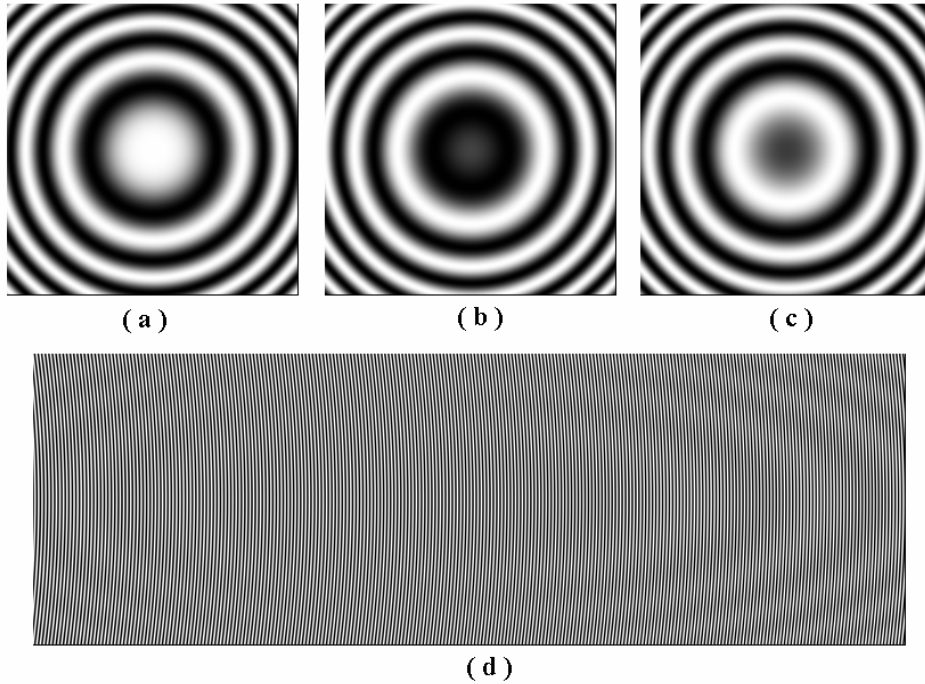


Fig. 2. Panels (a) (b) and (c) represents three phase shifted interferograms of a defocused wavefront. Panel 2(d) is the single spatial interferogram obtained using Eq. (3). Panel (d) is the carrier frequency interferogram with a spatial frequency of  $2\pi/3$  radians/pixel.

An example of this is shown in Fig. 2 where we show in panels 2(a), 2(b) and 2(c) three temporal phase shifted interferograms ( $\alpha = 2\pi/3$ ) and in panel 2(d) we show the single-image spatial-carrier frequency interferogram blended from the three above. As we can see from Eq. (3) and Fig. 2 we have merged into a single spatial dimension the temporal/phase coordinate  $\alpha$  and a spatial coordinate either  $x$  for Eq. (3) or  $y$  for Eq. (4). In Fig. 3 we can see that the phase  $\phi(x, y)$  obtained by combining the three fringe patterns (Panels 3(a), 3(b) and 3(c)) is constant over three consecutive pixels. This makes the phase of the newly obtained spatial fringe pattern to be stretched-out three times along the  $x$  coordinate (Panel 3(d)). In this way after demodulating the fringe pattern given by Eq. (3) we will take the central pixel as our estimated phase  $\phi(x, y)$ .

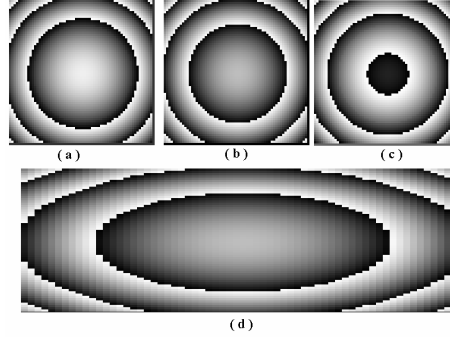


Fig. 3. Panels (a) (b) and (c) on this figure represent the shifted phase of the interferograms in Fig. 2. Panel (d) shows the blended modulating phase of interest  $\phi(x, y)$ . We can see that three consecutive pixels have the same value of modulating phase.

Generalizing this blending technique to  $M$ -PS interferograms we will obtain a single spatial carrier interferogram given by,

$$I'(Mx+m, y) = I(x, y, m\alpha), \quad \alpha = \frac{2\pi}{M}, \quad (0,0) < (x, y) < (L, L), \quad m = 0, \dots, M-1 \quad (4)$$

This fringe pattern representation may also be rewritten in a more familiar way as,

$$I'(x', y) = a(x', y) + b(x', y) \cos[\alpha x' + \phi(x', y)], \quad (0,0) < (x', y) < (ML, L), \quad \alpha = \frac{2\pi}{M} \quad (5)$$

The modulating phase  $\phi(x', y)$  is now a  $M$ -pixel piece-constant spatial function along the new  $x'$  coordinate as shown in panel 3(d). Using the mathematical expression in Eq. (5) we have increased the dimensionality of our fringe pattern in the  $x$  spatial direction, adding to it the temporal/phase dimension  $\alpha$  and obtaining a single fringe pattern of  $ML \times L$  dimensionality, so no data is lost nor gained with this re-arrangement of information.

As conclusion of this section we may say that the operator in Eq. (4) transforms a set of  $M$ -PS interferograms into a single carrier-frequency fringe pattern having a spatial carrier equals to  $\alpha = 2\pi/M$  radians and having an extended spatial support of  $(ML, L)$  pixels. Having this fringe pattern one may use a wider range of interferometric techniques such as  $N > M$  step phase stepping algorithms along the  $x'$  direction, or compact support spatial wavelets, or even straightforward whole field two-dimensional Fourier or Direct interferometry [6, 7].

### 3. Squeezed phase shifting interferometry

In this section we propose what we think it is a very efficient way to deal with our single carrier frequency interferogram of size  $(ML, L)$  given in Eq. (4). In this context we propose a

Gabor quadrature filter as a good choice to demodulate this fringe pattern. In particular the use of the following Gabor quadrature filter is suggested,

$$G_{\alpha}(x, y) = [\cos(\alpha x) + i \sin(\alpha x)] e^{-\left[ \frac{x^2}{(M\sigma)^2} + \frac{y^2}{\sigma^2} \right]}, \quad \alpha = \frac{2\pi}{M}. \quad (6)$$

Where  $\alpha$  is the phase shift among the  $M$  interferograms. Also the wider spread in the  $x$  direction ( $M\sigma$ ) in the Gabor quadrature filter  $G_{\alpha}(x, y)$  is due to the fact that the temporal axis was merged with the  $x$  axis in this case. In this way in order to obtain an spatially isotropic (in terms of the phase information  $\phi(x, y)$  in Eq. (1)) quadrature filter it is necessary to spread-out the  $x$  direction  $M$  times. Therefore to demodulate the single fringe pattern using  $G_{\alpha}(x, y)$  in Eq. (6) we only need to specify the spreading parameter  $\sigma$  to tune it up to our specific phase demodulating needs.

The formula (or phase shifting algorithm) to demodulate our  $M$  phase shifted interferograms is then,

$$\phi(x, y) = \arctan \left\{ \frac{\text{Im} [ I'(x, y) ** G_{\alpha}(x, y) ]}{\text{Re} [ I'(x, y) ** G_{\alpha}(x, y) ]} \right\}, \quad (0, 0) < (x, y) < (L, L), \quad (7)$$

where  $\phi(x, y)$  is the demodulated wrapped phase, and the operators  $\text{Im}(\cdot)$  and  $\text{Re}(\cdot)$  take the imaginary and real parts of the two-dimensional convolution product  $I'(x, y) ** G_{\alpha}(x, y)$ . As it is well known the spatial and frequency response of our  $G_{\alpha}(x, y)$  quadrature filter is a one sided Gaussian filter centered at the carrier frequency  $\alpha$  of the interferogram. As can be seen it is wider in the  $x$  direction where the temporal/phase axis was merged with the original  $x$  axes.

The Gabor quadrature filter may be isotropic (in the measuring phase  $\phi(x, y)$ ) as shown in Eq. (6) but it also can be made non-isotropic by changing the Gaussian spread along the  $x$  and/or  $y$  axis as follows,

$$G_{\alpha}(x, y) = [\cos(\alpha_x x) + i \sin(\alpha_x x)] e^{-\left[ \frac{x^2}{(M\sigma_x)^2} + \frac{y^2}{\sigma_y^2} \right]}, \quad \alpha = \frac{2\pi}{M}, \quad (8)$$

Using this Gabor filter we may vary the frequency response along the  $x+\alpha$  or the  $y$  direction. For example if we use ( $\sigma_x > \sigma_y$ ) we will have a smaller bandwidth in the  $x+\alpha$  direction, squeezing the noise in this coordinate more than in the  $y$  coordinate. Conversely, as we already mentioned, we may also combine our  $M$  phase shifted interferograms to obtain the following carrier frequency interferogram, having a size of  $LxML$  pixels,

$$I'(x, My + m) = I(x, y, m\alpha), \quad \alpha = \frac{2\pi}{M}, \quad (0, 0) < (x, y) < (L, L), \quad m = 0, \dots, M - 1 \quad (9)$$

In this case we have combined the temporal/phase coordinate with the  $y$  coordinate to obtain an interferogram having  $(x, y+m)$  as spatial coordinates. A Gabor filter  $G_{\alpha}(x, y)$  with a higher spread  $\sigma_x$  along the  $y+m$  coordinate may then be used. As we have just seen the fringe processing possibilities are highly increased using the proposed carrier frequency interferogram construction. Finally in the special case of a 3 step phase shifting interferograms the use of our proposed squeezing interferometry offers a much wider range of processing possibilities and with better signal to noise ratio than just the handful ones that we had if we had stayed with the traditional 3 step phase shifting interferometry.

#### 4. Numerical results

We now present two illustrative fringe processing examples to show the attractive possibilities of the herein proposed squeezing interferometric technique. We have used the Fourier space domain to calculate the phase given in Eq. (7) in all the examples presented in this paper.

Figure 4 shows a numerical experiment with 3 phase shifted noisy fringe patterns. The amount of phase shifting in these images is  $2\pi/3$  radians. In panel 4(a) we show a computer generated noisy interferogram (from the set of 3 phase shifted images) that was used to test the noise robustness of our proposed squeezing technique. Panel 4(b) shows the resulting wrapped phase image when a quadrature Gabor filter (Eq. (8)) of size  $(\sigma_x=1, \sigma_y=1)$  in the spatial domain was used. The deviation of the recovered phase with respect to the un-noisy phase for the PS 3 step algorithm is 1.1, while the standard deviation of the recovered phase with respect to the ideal phase for the squeezing technique is 0.21.

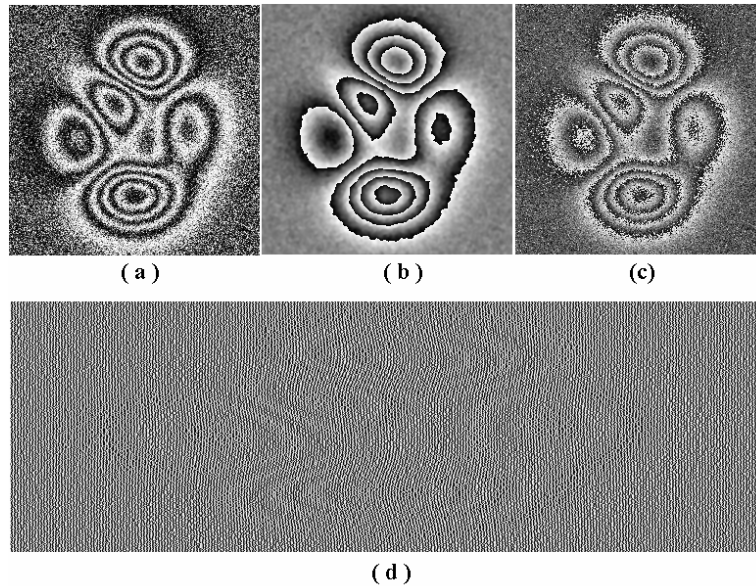


Fig. 4. Panel (a) shows a computer generated interferogram of a noisy phase, we have generated 2 additional phase shifted ( $\alpha=2\pi/3$ ) interferograms (not shown) with the same noisy phase. Panel (b) represents the estimated phase  $\hat{\phi}(x, y)$  obtained from demodulating the carrier frequency interferogram shown in Panel (d) and extracting only the “middle” pixel from the three consecutive pixels that have the same phase  $\phi(x, y)$ . Panel (c) shows the resulting estimated phase using the three step phase shifting algorithm in Eq. (2). We can see that the estimated phase in panel (c) has substantially more noise than the one shown in panel (b).

In Fig. 5 we show the same phase object shown in Fig. 4 but now we are testing the proposed algorithm for harmonic rejection so in this case our computer generated fringes are noiseless but fully saturated. Saturation modeling was obtained by binarizing the noiseless fringe patterns. In panels 5(a), 5(b), and 5(c) we show the 3 phase shifted binary fringe patterns and panel 5(c) shows the resulting saturated carrier fringe pattern obtained by the combination of the three phase shifted images above. Panel 5(b) shows the resulting wrapped phase image when a quadrature Gabor filter (Eq. (8)) of size  $(\sigma_x=2, \sigma_y=2)$  in the spatial domain was used. In this case the phase error deviation  $\sigma$  due to the harmonic content of the saturated fringes using the 3 step phase stepping algorithm is 0.4, while the corresponding phase error using the proposed squeezing technique is 0.13.

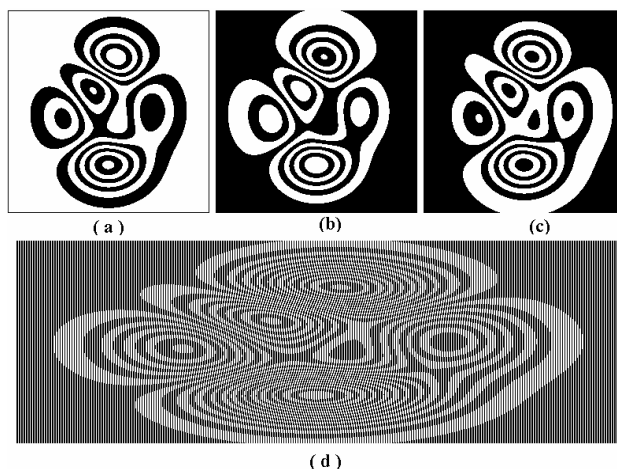


Fig. 5. In panels (a), (b), and (c) we show three phase shifted (with  $\alpha=2\pi/3$ ) interferograms which have been fully saturated to show the harmonic rejection capability of the squeezing interferometry technique. Panel (d) shows the blended carrier frequency fringe image obtained using the images in panels (a), (b) and (c).

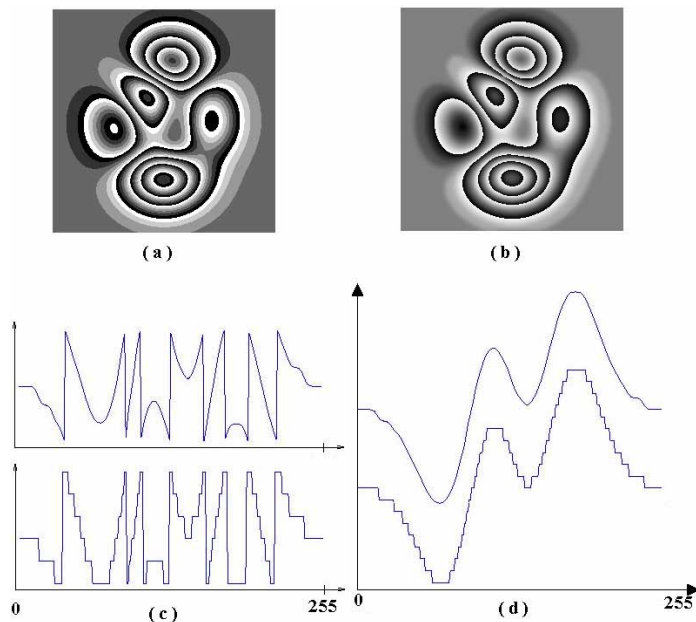


Fig. 6. Panel (a) shows the staircase phase obtained from the three saturated phase shifted interferograms shown in Fig. 5 and demodulated according to Eq. (2). Panel (b) shows the phase obtained (taking the “middle” phase value) from the carrier interferogram of Panel (d) in Fig. 5. We can see that the estimated phase using our proposed squeezing interferometric technique shown in panel (b) has less harmonic components than the one obtained using the standard 3 step phase shifting algorithm (Eq. (2)) shown in panel (a). Panel (c) shows gray level “cuts” of panels (a) and (b) to clearly show the difference between the two recovered wrapped phases. Panel (d) shows the same phase information as in panel (c) but now the phase “cuts” are shown unwrapped.

Finally Fig. 6 shows the resulting phase obtained using the standard 3 step interferometry against our proposed method. Panel 6(a) shows the wrapped phase obtained by using the 3 step PSI in Eq. (2), we may see that the resulting phase is a staircase spatial function having

only six discrete phase values in the interval  $[0, 2\pi]$  radians. On the other hand in panel 6(b) we show the resulting phase when squeezing interferometry was used. Here we can see that our phase map looks much smoother. The quadrature Gabor filter used in this case is the same as the one used to obtain the wrapped phase in panel 4(b) above. Finally in panels 6(c) and 6(d) we show a line cut through the wrapped and unwrapped phases to clearly see their difference. As mentioned, the phase obtained using the 3 step PSI algorithm markedly behaves as a staircase function while our squeezing technique has a much better harmonic rejection.

## 5. Conclusion

We have presented a simple, yet powerful way of spatially re-distributing a set of  $M$ -PS interferograms of size  $(L, L)$  to obtain a single-image spatial-carrier fringe pattern having a spatial support of  $ML \times L$  and a carrier frequency of  $\alpha = 2\pi/M$ . As far as we know this simple, yet efficient way of redistributing the data in order to have more processing flexibility has not yet been reported. The herein presented method has several advantages over a simple  $M$ -step phase shifting interferometry, in the sense that we may use not just a  $M$ -step discrete phase formula, but we also may use a “phase shifting formula” in terms of Gabor quadrature filters with any desired (given by a real number) spatial/frequency spread in either the  $x+\alpha$  or  $y$  axis. A consequence of this is a higher signal to noise ratio of the estimated phase, and better harmonic rejection than a simple  $M$ -step phase shifting algorithm.

Putting this in other words, we have proposed a new way of blending the temporal synchronous method [8] with the spatial synchronous methods [6, 7]. Our squeezing technique provides the user with a single image having the spatio-temporal information provided by  $N$  phase-stepped fringe patterns. This way of combining information is (as far as we know) new. A final and important remark may be given at this point; one can always figure out a series of ad-hoc processing techniques to give an “equivalent” demodulation results as the ones given in this paper. But this “equivalent” method will certainly have a more cumbersome processing strategy, and the user would not gain any better insight into the problem.

Finally, using a Gabor filter with non-isotropic spatial spread along one of the new spatial coordinates  $(x+\alpha, y)$  we may squeeze the frequency response of one spatial coordinate over the other. In this way we may design a continuously band-width quadrature filter to fulfill any special need that may arise in a given experiment. Using the proposed technique of rearranging the interferogram’s information one may also try other kind of quadrature filtering such as wavelets or windowed Fourier transforms to demodulate the  $M$  phase shifted interferograms.

## Acknowledgments

The authors want to acknowledge the support of the Consejo Nacional de Ciencia y Tecnologia de Mexico (CONACYT).